# Insight into the Enzyme–Inhibitor Interactions of the First Experimentally Determined Human Aromatase

**Article** *in* Journal of Biomolecular Structure and Dynamics · April 2011

DOI: 10.1080/07391102.2011.10508604 · Source: PubMed

CITATIONS
5

READS
250

**3 authors:**

Ankita Punetha
Rutgers New Jersey Medical School
**22** PUBLICATIONS **414** CITATIONS
SEE PROFILE

Karthi Shanmugam
SASTRA University
**36** PUBLICATIONS **673** CITATIONS
SEE PROFILE

Durai Sundar
Indian Institute of Technology Delhi
**181** PUBLICATIONS **4,448** CITATIONS
SEE PROFILE

*Journal of Biomolecular Structure & Dynamics, ISSN 0739-1102*
*Volume 28, Issue Number 5, (2011)*


# Insight into the Enzyme-Inhibitor Interactions of the First Experimentally Determined Human Aromatase

http://www.jbsdonline.com

**Ankita Punetha[1]**
**Karthi Shanmugam[1,2]**
**Durai Sundar[1]***

[1]Department of Biochemical Engineering and Biotechnology, Indian Institute of Technology (IIT) Delhi, Hauz Khas, New Delhi 110016, India
[2]Department of Bioinformatics, School of Chemical and Biotechnology. SASTRA University, Tirumalaisamudram, Thanjavur 613402 Tamil Nadu, India

***Abstract***

Aromatase is an important pharmacological target in the anti-cancer therapy as the intratumoral aromatase is the source of local estrogen production in breast cancer tissues. Suppression of estrogen biosynthesis by aromatase inhibition represents an effective approach for the treatment of hormone-sensitive breast cancer. Because of the membrane-bound character and heme-binding instability, no crystal structure of aromatase was reported for a long time, until recently when crystal structure of human placental aromatase cytochrome P450 in complex with androstenedione was deposited in PDB. The present study is towards understanding the structural and functional characteristics of aromatase to address unsolved mysteries about this enzyme and elucidate the exact mode of binding of aromatase inhibitors. We have performed molecular docking simulation with twelve different inhibitors (ligands), which includes four FDA approved drugs; two flavonoids; three herbal compounds and three compounds having biphenyl motif with known $IC_{50}$ values into the active site of the human aromatase enzyme. All ligands showed favorable interactions and most of them seemed to interact to hydrophobic amino acids Ile133, Phe134, Phe221, Trp224, Ala306, Val370, Val373, Met374 and Leu477 and hydrophilic Arg115 and neutral Thr310 residues. The elucidation of the actual structure-function relationship of aromatase and the exact binding mode described in this study will be of significant interest as its inhibitors have shown great promise in fighting breast cancer.

Key words: Aromatase; breast cancer; cytochrome P450 enzyme; molecular docking; androstenedione; aromatase inhibitors; aminoglutethimide; anastrozole; fadrozole; letrozole; estrogen

## *Introduction*

Breast cancer is the most common form of cancer among women in Europe, North and South America and Australasia; approximately one-in-ten in Western countries are diagnosed with breast cancer at some point in their life (1) and 50-80% of these suffer tumours that are estrogen-dependent (2) with the tumour cells expressing estrogen receptors, and the growth of the tumours being stimulated by circulating estrogen. The incidence of breast cancer is increasing on average by about 1% per year in industrialized countries and at a greater rate in developing countries. A number of factors are recognized which increase a woman's risk of developing the disease. Genetic predisposition, or family history of breast cancer, is known to be responsible for 5% of all cases. However, the variation in incidence throughout populations, and changes relating to population migration and adoption of altered lifestyles, all point to the critical importance of nongenetic determinants.

The estrogen-dependent mammary carcinomas can be combated through selectively depriving the body of estrogen by ovariectomy in pre-menopausal women

*Phone: +91-11-26591066
Fax: +91-11-26582282
E-mail: sundar@dbeb.iitd.ac.in

or by the use of anti-estrogens (like tamoxifen), that interfere with the binding of estrogen to its receptor, or else through the use of pharmacological inhibitors of estrogen production. Two circulating estrogens-estrone and estradiol-are produced from cholesterol (Figure 1). Inhibiting the enzymes that are involved at earlier steps in the branching pathway of steroidogenesis could have an undesirable impact on the production of other physiologically important hormones such as aldosterone and cortisol. Since aromatase catalyzes the last step in estrogen production, the conversion of androgens - androstenedione and testosterone to the aromatic estrogenic steroids estrone and estradiol, respectively, through the aromatization of the A-ring of the substrate, it serves as an ideal target for the development of selective and potent inhibitors. Aromatase inhibitors, act to decrease the circulating levels of estrogen by blocking the biosynthesis of the compound from androgens (3). Aromatase inhibitors therefore constitute a frontline therapy for oestrogen-dependent breast cancer (3, 4).

Potential lead compounds with molecular structural features that are related to biological activity can be identified by computer-aided drug design. Structure-based explorations have been applied to study ligand and receptor interaction and have been applied in drug design (5-14). There has been development of new scoring function (15) and successful implementation of computer-aided drug design into development of new therapeutics (16-19). Thus, one is in a good position to apply such technologies to develop well designed inhibitors of aromatase.

The *CYP19* gene is localized at chromosome 15q21.2 that encodes aromatase (EC 1.14. 14.1) (20) and is produced to high levels in breast tissue, and particularly in those areas in and around tumour sites (3). Competitive aromatase inhibitors are molecules that compete with the substrate androstenedione for noncovalent binding to the active site of the enzyme to decrease the amount of product formed. Mechanism-based aromatase inhibitors are steroidal inhibitors that mimic the substrate, are converted by the enzyme to a reactive intermediate, and result in the inactivation of aromatase. Steroidal inhibitors that have been developed to date are built upon the basic androstenedione nucleus and incorporate chemical substituents at varying positions on the steroid. Non-steroidal aromatase inhibitors can be divided into three classes: aminoglutethimide- like molecules, imidazole/triazole derivatives, and flavonoid analogs. Both steroidal and non-steroidal aromatase inhibitors have shown clinical efficacy in the treatment of breast cancer. The requirement for even more potent and selective inhibitors led to intensive molecular studies to identify the structure of

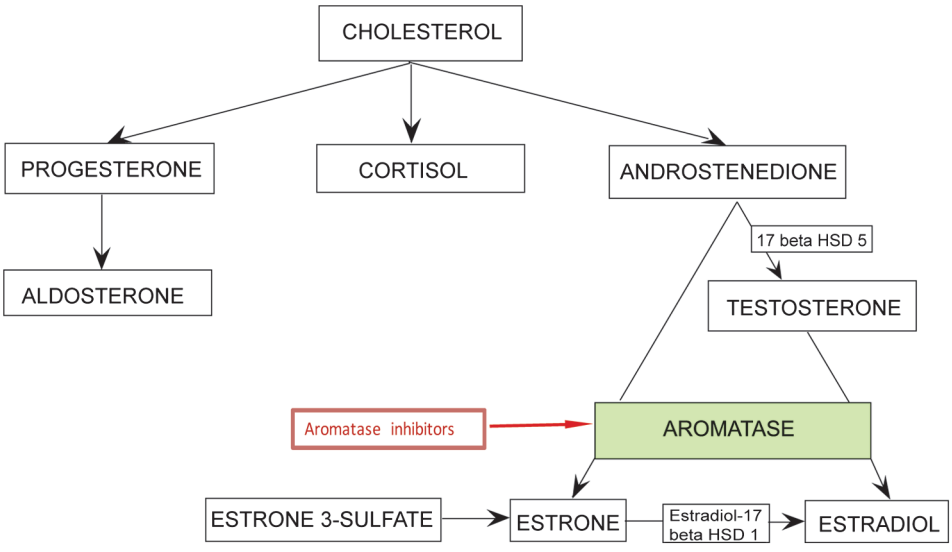


**Figure 1:** The biosynthesis of estrogen from cholesterol. Trace back into the history. The role of aromatase in estrogen synthesis is in catalyzing the conversion of androgens-androstenedione and testosterone to the aromatic estrogenic steroids-estrone and estradiol, respectively.

aromatase, to development of the third-generation aromatase inhibitors, letrozole, anastrozole, and exemestane, which are now licensed for clinical use in the treatment of metastatic estrogen-dependent breast cancer in post-menopausal women. Other known inhibitors of the enzyme include various flavonoid compounds, in particular those based on the flavone and flavanone skeletons (3, 21). These compounds have attracted considerable interest in regard to aromatase inhibition, in part because of the hypothesis put forward that these natural products may represent dietary factors that account for the significantly lower incidence of breast cancer amongst women of Asian and Oriental origin (22) and also because of the reported general inverse association between the incidence of breast cancer and consumption of flavonoid-rich vegetables (23-25). The aromatase inhibitors can be highly effective in treatments of breast cancer and for use in reproductive disorders.

*Structure of Aromatase Reveals Secrets of Selective Inhibition*

Aromatase is a cytochrome P450 enzyme, consisting of a haem group and a polypeptide chain of 503 amino-acid residues and forms an electron-transfer complex with its partner, NADPH-cytochrome P450 reductase. The 2.90 Å resolution crystal structure of aromatase purified from human placenta in complex with its natural substrate androstenedione (androst-4-ene-3, 17-dione) exhibits the characteristic cytochrome P450 fold. The residues comprising the catalytic cleft are Ile 305, Ala 306, Asp 309 and Thr 310 from the I-helix, Phe 221 and Trp 224 from the F-helix, Ile 133 and Phe 134 from the B-C loop, Val 370, Leu 372 and Val 373 from the K-helix–b3 loop, Met 374 from b3, and Leu 477 and Ser 478 from the b8–b9 loop. The volume of the binding pocket is around 400 $Å^3$, considerably smaller than the volume of about 530 $Å^3$ of the active sites in human P450s with highest sequence identities (14–18%) to human aromatase (26). Whereas most P450s are not highly substrate selective, it is the hallmark androgenic specificity that sets aromatase apart. Earlier docking studies have been performed using the aromatase modelled structure [PDB: 1TQA]. We performed the docking studies using the experimentally determined structure 3EQM deposited in the PDB in the year 2009 (26). In the work reported here, we have used the structural data of the already known aromatase inhibitors and have performed molecular docking studies to gain insight into the difference in binding mode of these inhibitors with the crystal structure of human placental aromatase, the only natural mammalian, full-length P450 and P450 in hormone biosynthetic pathways to be crystallized so far.

## *Materials and Methods*

*Preparation of Ligands for Molecular Docking*

The set of ligand molecules studied in this work include four FDA approved drugs Aminoglutethimide [PubChem: CID 86488], Anastrozole [PubChem: CID: 2187], Fadrozole [PubChem: CID 59693], Letrozole [PubChem: CID 3902](27); two flavonoids – flavone and isoflavone (28); three herbal compounds Gossypetin, Liquiritigenin and Myricetin (29) and three compounds having biphenyl motif with known $IC_{50}$ values (2-{5-[(1H-1,2,4-Triazol-1-yl)methyl]biphenyl-3-yl}-2-methyl-propionitrile; 6-[(1H-1,2,4-Triazol-1-yl) methyl]biphenyl-3-carbonitrile; 1-(Biphenyl-4- ylmethyl)-1H-1,2,4-Triazole) (30). These ligand molecules were retrieved from the various published literature on aromatase inhibitors (28-30). The structure of these compounds were built and optimized with ChemSketch software suite (ver 11.02) and ChemDraw Ultra (ver 9.0). The energy of the ligands was minimized using CHARMm force field in Discovery Studio 2.1. The algorithm used for minimization was conjugate gradient with minimization carried out for 10,000 steps using implicit solvent model Generalized Born with a simple switching and their structures are shown in Figure 2.

The three dimensional structure of human placental aromatase at 2.9Å [PDB:3EQM] was obtained from Protein Data Bank (PDB) (31). This structure has been originally determined using x-ray diffraction (26). This human aromatase enzyme structure is complexed with ligand androstenedione and water molecules. Protein

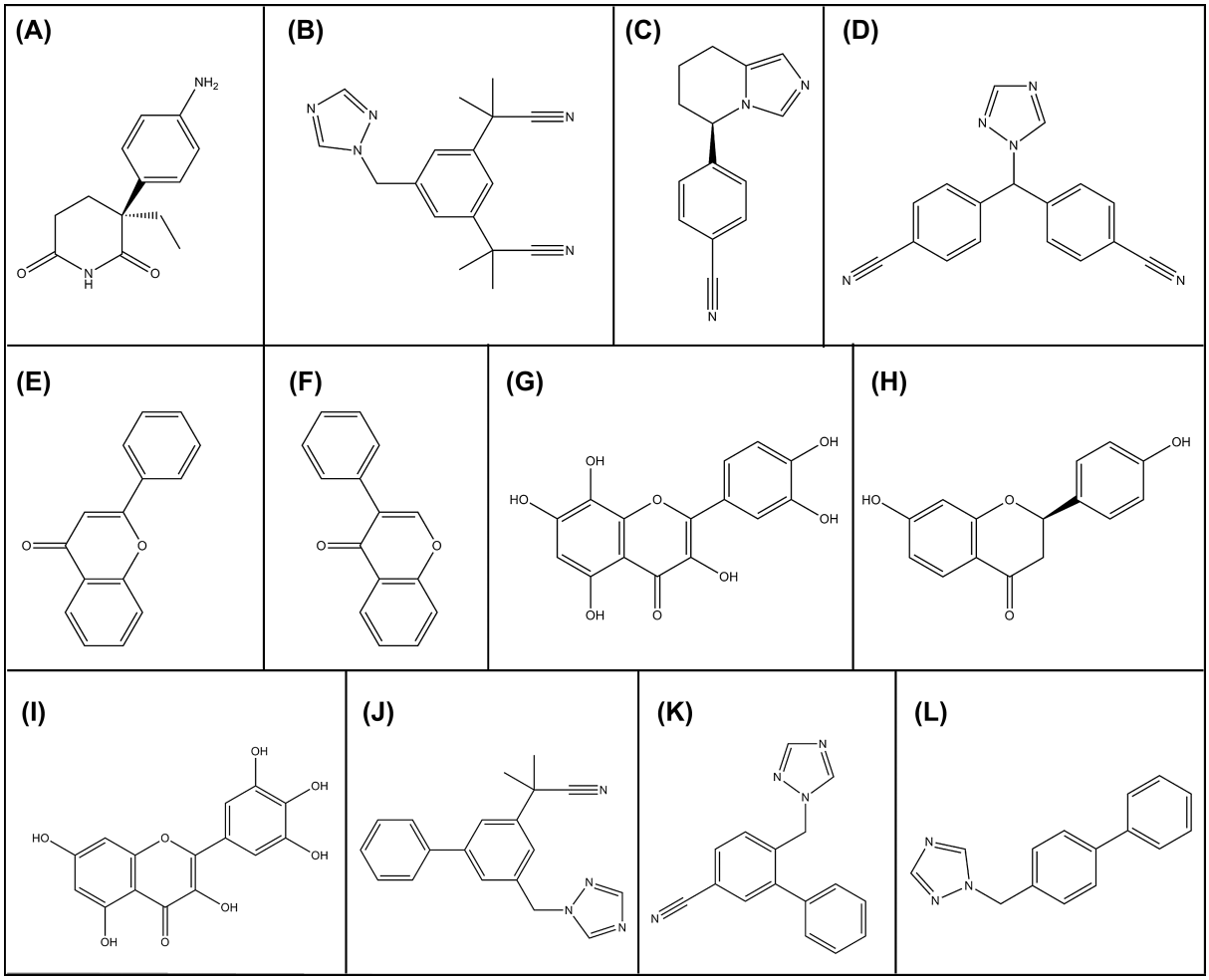


**Figure 2:** Two dimensional molecular structures of the ligands/inhibitors. (**A**) Aminoglutethimide, (**B**) Anastrozole, (**C**) Fadrozole, (**D**) Letrozole, (**E**) Flavone, (**F**) Isoflavone, (**G**) Gossypetin, (**H**) Liquiritigenin, (**I**) Myricetin, (**J**) 2-{5-[(1H-1,2,4-Triazol-1-yl)methyl]biphenyl-3-yl}-2-methylpropionitrile, (**K**) 6-[(1H-1,2,4-Triazol-1-yl)methyl]biphenyl-3-carbonitrile, (**L**) 1-(Biphenyl-4-ylmethyl)-1H-1,2,4-Triazole.

preparation was done by removing the ligand and the solvent molecules from the PDB file and a free receptor was made. Hydrogen atoms were added to target protein atom and proper protonation states were assigned to each of the residues to correct ionization and tautomeric states of amino acid residues. Since heme is also a part of the aromatase, proper charges were assigned to it and heme was set to a (IV) protonation state (26). Harmonic constraint was applied to restrain the positions of atoms in the space before proceeding for minimization. The energy of the target aromatase was minimized in Steepest Descent followed by Conjugate Gradient method using Accelrys Discovery Studio (Version 2.1, Accelrys Software Inc.), the most comprehensive suite of modeling and simulation solutions for drug discovery available (Table I). The algorithm used for minimization was steepest descent followed by conjugate gradient. Each of the minimization methods were carried out with CHARMm force field with 10,000 minimization steps using implicit solvent. Implicit solvent model used was Generalized Born with a simple switching (GBSW) to give a better approximation for the solvent effect.

In order to carry out the docking simulation, we used the AutoDock 4.0 suite as molecular-docking tool (32). Several studies report the comparison of AutoDock with various docking programs. Autodock has been found to be able to locate docking modes that are consistent with X-ray crystal structures (33, 34). Autodock helps to simulate interactions between substrates or drug candidates as ligands and their macromolecular receptors of known three dimensional structures, allowing ligand flexibility described to a full extent elsewhere (35). It is

**Table I**
Summary of energy minimization of protein human aromatase.

| | Energy levels after Steepest Descent (kcal/mol) | | | | Energy levels after Conjugate Gradient (kcal/mol) | | | |
|---|---|---|---|---|---|---|---|---|
| Molecule | Int PE | PE | VdwE | EE | Int PE | PE | VdwE | EE |
| Human placental aromatase (3eqm) | –16235.61 | –23839.14 | –3738.87 | –17081.84 | –23839.14 | –24232.52 | –3808.47 | –17238.04 |

suitable software for performing automated docking of ligands to their macromolecular receptors. In this docking simulation, we used semi-flexible docking protocols. In the target protein aromatase the residues Arg115, Asp309, Met374 were given flexibility as they are known to be involved in the interaction with the substrate while the ligands being docked were kept flexible, in order to explore an arbitrary number of torsional degrees of freedom in addition to the six spatial degrees of freedom spanned by the translational and rotational parameters. The Graphical User Interface program "AutoDock Tools" was used to prepare, run, and analyze the docking simulations. Kollman united atom charges, solvation parameters were added into the receptor PDB file for the preparation of protein in docking simulation. Since ligands are not peptides, Gasteiger charge was assigned and then non-polar hydrogens were merged. The rigid roots of each ligand were defined automatically instead of picking manually. Auto-Tors, an auxiliary program using Interactive queries to define rotatable torsion angles, is used to assign all rotatable dihedrals in the ligands and to remove non-polar hydrogen atoms, uniting their partial charges with their bonded carbon atoms. All rotable dihedrals in the ligands were assigned with the help of Auto-Tors and were allowed to rotate freely. AutoDock requires pre-calculated grid maps, one for each atom type, present in the ligand being docked. AutoGrid, which calculates grids of interaction energy based on the interaction of the ligand atom probes with receptor target, is used to obtain the grid maps required prior to docking. Each probe consists of an atom type present in the ligand being docked. The pre-calculated grid maps store the potential energy arising from the interaction with the macromolecule. The user defined three dimensional grid must surround the region of interest in the macromolecule, and the ligand was limited to this search space during docking. In the present study, the location and dimensions of grid box are chosen such that it incorporates the amino acid stretch of aromatase involved in binding with the natural substrate androstenedione for the formation of aromatse-androstenidione complex as revealed by experimental studies (26). The energy scoring grid was prepared as a 60, 60, and 60 Å (x, y, and z) cube. The spacing between grid points was 0.375 angstroms. Arg115, Asp309 and Met374 were selected as active residues during the preparation of grid parameter file. Atomic solvation parameters were assigned to the receptor using default parameters. The Lamarckian Genetic Algorithm (LGA) was chosen to search for the best conformers. Using mathematical concepts designed to simulate the conditions influencing biological evolution, genetic algorithms are able to search conformational space by "mutating" a ligand in order to find its lowest energy conformation in the "environment" of a fixed protein. Searches driven by this energy funnelling have been shown to provide a good indication

as to the optimum protein-ligand interaction and therefore the structure most likely to be found *in vivo* (36). Thus, genetic algorithm is a search heuristic that generate solutions to optimization problems by mimicking the process of natural evolution such as inheritance, mutation, selection, and crossover. The most important idea is that a population of individuals interacts through genetic operators to carry out an optimization process. The evolution starts from a population of randomly generated individuals and happens in generations. In each generation, the fitness of every individual in the population is evaluated; multiple individuals are stochastically selected from the current population and modified to form a new population. The new population is then used in the next iteration of the algorithm. The algorithm terminates when either a maximum number of

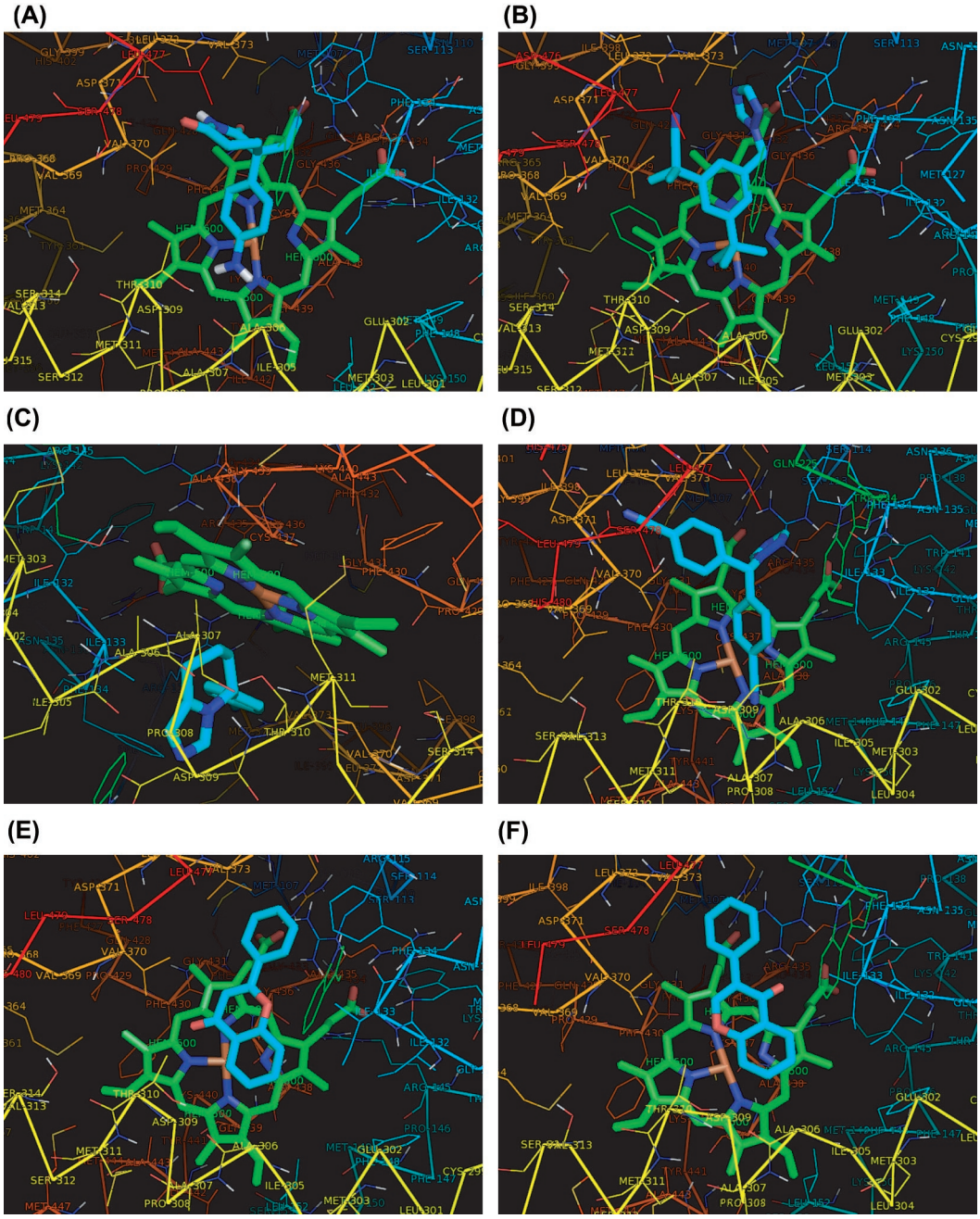


**Figure 3:** Representative docking models of various inhibitors. (**A**) Aminoglutethimide, (**B**) Anastrozole, (**C**) Fadrozole, (**D**) Letrozole, (**E**) Flavone, (**F**) Isoflavone, (**G**) Gossypetin, (**H**) Liquiritigenin, (**I**) Myricetin, (**J**) 2-{5-[(1H-1,2,4-Triazol-1-yl)methyl]biphenyl-3-yl}-2-methylpropionitrile, (**K**) 6-[(1H-1,2,4-Triazol-1-yl)methyl]biphenyl-3-carbonitrile, (**L**) 1-(Biphenyl-4-ylmethyl)-1H-1,2,4-Triazole into aromatase enzyme. All the amino acid residues which are surrounding the ligand are shown in wire frame drawing. Ligands and the haem in the aromatase structure are shown in stick drawing.

generations has been produced, or a satisfactory fitness level has been reached for the population. The default parameters for the Lamarckian genetic algorithm (35) were used as the search protocol except for the maximum number of energy evaluations, which were changed to 2.5. During the docking process, a maximum of 10 conformers was considered for each compound. The population size was set to 150 and the individuals were initialized randomly. Maximum number of generations was kept as 27000, maximum number of top individual that automatically survived set to 1, mutation rate of 0.02, crossover rate of 0.8. Step sizes for translations, quaternion and torsions were kept same as defaults. 10 LGA runs were performed with Cluster tolerance 0.5 Å, external grid energy 1000.0, max initial energy 0.0 and 10000 max number of retries.

An efficient and accurate energy assessment of the ligand conformations is as important to the success of a docking simulation as the power of the search

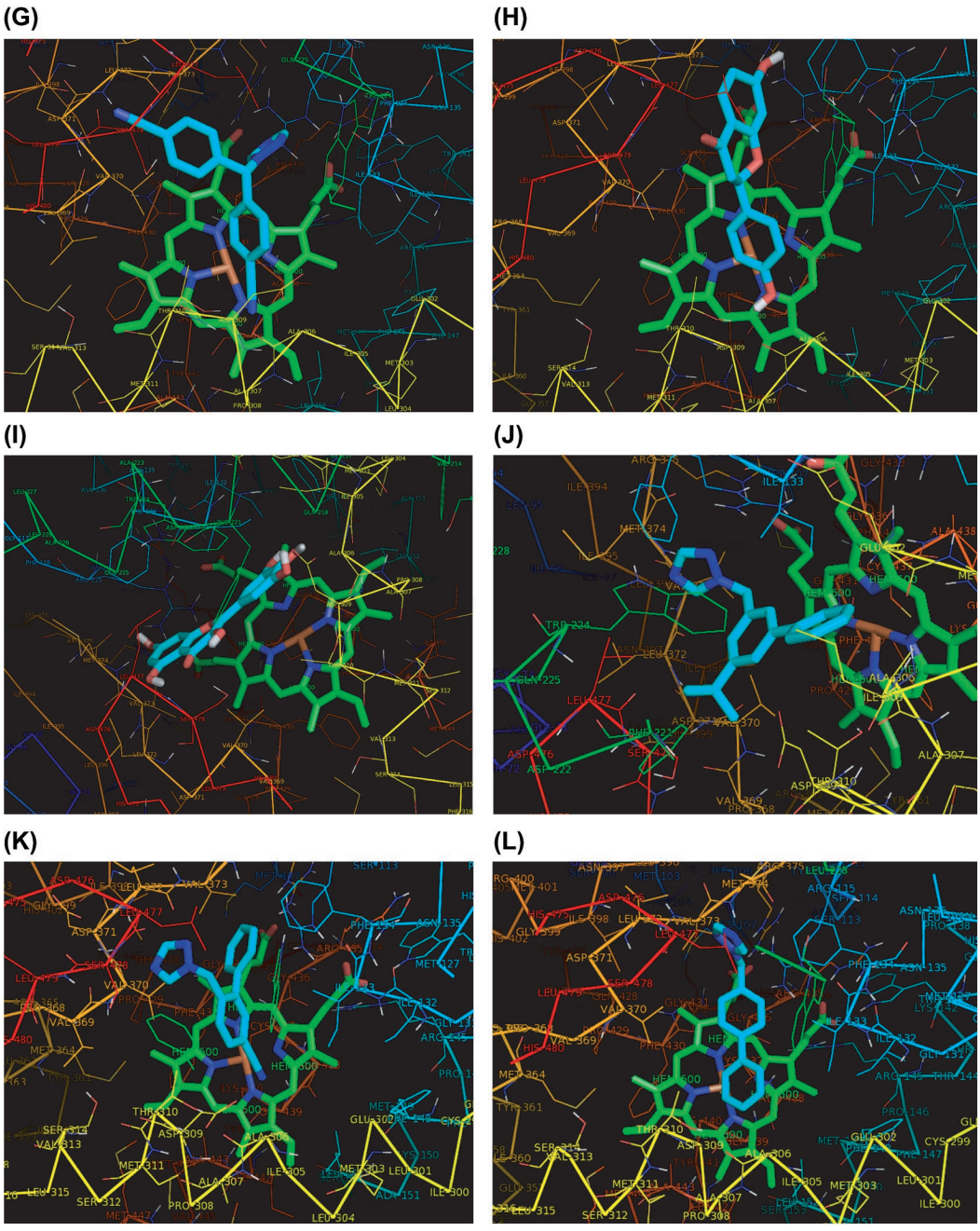


**Figure 3:** *(Continued)*

algorithm. AutoDock uses a variation on the AMBER'95 force field (37) with terms empirically determined by linear regression analysis from a set of protein-ligand complexes with known binding constants (35, 38). Gibbs Free energy (ΔG) is calculated as a sum of six energy terms of dispersion/repulsion, hydrogen bonding, electrostatic interactions, deviation from covalent geometry, internal ligand torsional constraints, and desolvation effects.

AutoDock reports the best docking solution (lowest docked free energy) for each GA run and also performs a cluster analysis in which the total number of clusters and the rank of each docking mode (cluster rank) are reported. Docking modes were selected on the basis of two criteria: their proximity to the active side residues and extent of the molecule's interactions with the interacting hydrophobic amino acid side chains of aromatase. So, for a 10 GA run, for example, there would be up to 10 total docking modes from which we chose the lowest energy-docking mode that met the above two criteria. The output from AutoDock and all modeling studies as well as images were rendered with PyMOL. All the AutoDock docking runs were performed in Velocis server having Intel Xeon Processor @ 3.0 GHz, with 8 GB RAM. AutoDock 4.0 was compiled and run under SUSE ENTERPRISE LINUX 10 operating system.

***Results and Discussion***

The close examination of the X-ray Diffraction structure of the human placental aromatase along with its substrate showed that the Pro308 residue causes a distortion in the I-helix backbone resulting in displacement of the helix axis which is further stabilized by a strong Ala306 CO…HO Thr310 (2.8 Å) hydrogen bond interaction. This Pro 308 (residue unique to aromatase among all P450's) - mediated axis shift precisely accommodates the 3-keto end of androstenedione allowing the Asp 309 side chain to hydrogen-bond to the 3-keto oxygen. The criteria which we followed in the selection of ligands include the known aromatase inhibitors already in clinical use plus the potent aromatase inhibitors with known inhibition values i.e. $IC_{50}$ values. Investigational aromatase inhibitors including the FDA-approved drugs such as Aminoglutethimide, Anastrozole, Fadrozole, Letrozole were retrieved from PubChem database and rest of the ligands were identified from literature. The final potential energy of aromatase taken for simulation was -24232.525 kcal/mol (Table I). Molecular docking simulations were conducted with the AutoDock 4.0 software suite. Ten docking runs were performed for each of the twelve different ligands into redox-active site of aromatase protein and the most stable docked complexes are shown in Figure 3. To verify the accuracy of the AutoDock 4.0 results, we also considered some top clusters of conformations/orientations in addition to the best scored one. In this molecular docking study, prediction was considered successful if the RMSD value is less than 2.0 Å for the best-scored conformation (39). The natural substrate androstenedione was also docked with prepared receptor to check the efficiency of the Autodock and effectiveness of the docking studies. The RMSD deviation between the original ligand position and the conformers obtained in the autodock came only to be 0.4 Å, thus validating the accuracy of docking program.

*Docking of Androstenedione into Aromatase*

The re-docking Androstenedione into aromatase resulted in only one conformational cluster having ten conformers (Table II). Fourth run had the lowest energy among all other docked conformations with the binding energy of -17.15 kcal/mol. In this docked complex, there were three polar contacts involving Arg115, Asp309, Met374 residues at 3.00 Å, 3.49 Å and 2.94 Å respectively. The residues involved in the polar contacts were in accordance with the literature. In addition to polar interactions, residues Phe134, Trp224 and Thr310 were involved in van der Waals interactions further stabilized the ligand (Table III).

Three different docked clusters were observed with flavone for aromatase (Table II). The tenth run had the lowest binding energy of -14.84 kcal/mol in the cluster rank1. There was no polar contact between flavone and aromatase. It was observed that the residues Ile133, Thr310, Val370 and Met374 were taking part in van der Waals interactions (Table III).

**Table II**
Summary of docking for natural substrate and top five ligands into protein human aromatase having lowest binding energy.

| Molecules | Number of distinct conformational clusters found | Number in cluster | Docking statistics (RMSD-tolerance of 2.0 Å) | | | |
|---|---|---|---|---|---|---|
| | | | Cluster rank | Lowest binding energy (kcal/mol) | Run | Cluster RMSD |
| Androstenedione | 1 | 10 | 1 | –17.15 | 4 | 0.00 |
| | | | 1 | –16.86 | 3 | 0.59 |
| | | | 1 | –16.72 | 10 | 0.40 |
| | | | 1 | –16.71 | 9 | 0.37 |
| | | | 1 | –16.53 | 6 | 0.47 |
| | | | 1 | –16.26 | 5 | 0.27 |
| | | | 1 | –16.06 | 8 | 1.54 |
| | | | 1 | –16.03 | 2 | 0.53 |
| | | | 1 | –15.37 | 1 | 1.57 |
| | | | 1 | –14.76 | 7 | 1.57 |
| Flavone | 3 | 8 | 1 | –14.84 | 10 | 0.00 |
| | | | 1 | –14.93 | 5 | 1.46 |
| | | | 1 | –13.77 | 4 | 1.42 |
| | | | 1 | –13.55 | 8 | 1.70 |
| | | | 1 | –12.94 | 3 | 1.70 |
| | | | 1 | –12.70 | 6 | 1.47 |
| | | | 1 | –12.67 | 2 | 0.35 |
| | | | 1 | –12.42 | 7 | 1.27 |
| | | 1 | 2 | –11.38 | 1 | 0.00 |
| | | 1 | 3 | –10.56 | 9 | 0.00 |
| 6-[(1H-1,2,4-Triazol-1-yl)methyl]biphenyl-3-carbonitrile | 3 | 7 | 1 | –14.76 | 4 | 0.00 |
| | | | 1 | –14.64 | 1 | 0.09 |
| | | | 1 | –14.62 | 5 | 0.13 |
| | | | 1 | –14.02 | 6 | 1.79 |
| | | | 1 | –13.92 | 10 | 0.69 |
| | | | 1 | –13.53 | 2 | 0.85 |
| | | | 1 | –12.89 | 8 | 1.55 |
| | | 2 | 2 | –12.40 | 7 | 0.00 |
| | | | 2 | –11.65 | 9 | 1.57 |
| | | 1 | 3 | –12.25 | 3 | 0.00 |
| 1-(Biphenyl-4-ylmethyl)-1H-1,2,4-Triazole | 5 | 1 | 1 | –14.72 | 6 | 0.00 |
| | | 3 | 2 | –13.77 | 5 | 0.00 |
| | | | 2 | –13.58 | 7 | 1.90 |
| | | | 2 | –13.27 | 4 | 1.95 |
| | | 3 | 3 | –13.26 | 8 | 0.00 |
| | | | 3 | –12.49 | 9 | 1.44 |
| | | | 3 | –12.05 | 3 | 0.67 |
| | | 2 | 4 | –12.91 | 2 | 0.00 |
| | | | 4 | –12.59 | 10 | 1.11 |
| | | 1 | 5 | –10.69 | 1 | 0.00 |
| 2-{5-[(1H-1,2,4-Triazol-1-yl)methyl]biphenyl-3-yl}-2-methylpropionitrile | 4 | 5 | 1 | –14.37 | 2 | 0.00 |
| | | | 1 | –13.81 | 6 | 1.41 |
| | | | 1 | –13.49 | 3 | 1.79 |
| | | | 1 | –10.92 | 5 | 1.68 |
| | | | 1 | –10.11 | 10 | 1.45 |
| | | 1 | 2 | –12.91 | 8 | 0.00 |
| | | 1 | 3 | –12.14 | 4 | 0.00 |
| | | 3 | 4 | –11.98 | 9 | 0.00 |
| | | | 4 | –11.51 | 7 | 1.06 |
| | | | 4 | –11.20 | 1 | 1.09 |

*Docking of 6-[(1H-1,2,4-Triazol-1-yl)methyl]biphenyl-3-carbonitrile into Aromatase*

The number of docked clusters observed with 6-[(1H-1,2,4-Triazol-1-yl) methyl] biphenyl-3-carbonitrile for aromatase produced three different clusters (Table II). The fourth run had the lowest binding energy of -14.76 kcal /mol. There was one polar contact between 6-[(1H-1,2,4-Triazol-1-yl)methyl]biphenyl-3-carbonitrile

**Table III**
Molecular interactions all the ligands into protein human aromatase.

| S.No. | Molecules | Residues involved in Polar interactions | Length of hydrogen bond (Å) | Residues involved in van der Waals interaction |
|---|---|---|---|---|
| 1 | Androstenedione | Arg115 | 3.00 | Phe134, Trp224, Thr310 |
| | | Asp309 | 3.49 | |
| | | Met374 | 2.94 | |
| 2 | Aminoglutethimide | none | none | Trp224, Val370, Leu372, Ala306 |
| 3 | Anastrazole | Thr310 | 3.25 | Arg115, Phe134, Met374, Trp224 |
| | | Ser478 | 3.51 | |
| 4 | Fadrozole | Ala306 | 2.92 | Met374, Arg115, Trp224, Phe221, Thr310, Asp309 |
| | | Thr310 | 2.78 | |
| | | Leu477 | 2.77 | |
| 5 | Letrozole | Leu372 | 2.75 | Val370, Ala306, Phe134, Arg115 |
| 6 | Flavone | none | none | Val370, Thr310, Ile133, Met374 |
| 7 | Isoflavone | none | none | Val370, Leu372, Phe134, Ile133, Ala306 |
| 8 | Gossypetin | Arg115 | 3.25 | Leu372, Trp224, Phe134, Val370 |
| | | Leu372 | 2.75 | |
| | | Met374 | 2.83 | |
| | | Leu477 | 2.97 | |
| 9 | Liquiritigenin | Leu477 | 2.63 | Leu477, Thr310, Phe134, Trp224 |
| | | Met374 | 2.98 | |
| 10 | Myricetin | Asp309 | 2.91 | Leu372, Ala306, Ile133 |
| | | Thr310 | 2.93 | |
| | | Leu477 | 3.08 | |
| 11 | 2-{5-[(1H-1,2,4-Triazol-1-yl)methyl] biphenyl-3-yl}-2-methylpropionitrile | Ala306 | 3.3 | Trp224, Ser478, Val370, Phe221, Phe134, Met374 |
| | | Thr310 | 3.19 | |
| | | Leu372 | 2.78 | |
| | | Leu477 | 2.74 | |
| 12 | 6-[(1H-1,2,4-Triazol-1-yl)methyl] biphenyl-3-carbonitrile | Leu477 | 3.06 | Asp309, Thr310, Met374, Phe134 |
| 13 | 1-(Biphenyl-4- ylmethyl)-1H-1,2,4-Triazole | none | none | Phe134, Thr310, Leu477 |

and Leu477 residue of aromatase, with bond length of 3.06 Å. It was observed that the residues Asp309, Thr310, Met374 and Phe134 were taking part in van der Waals interactions (Table III).

*Docking of 1-(Biphenyl-4-ylmethyl)-1H-1,2,4-Triazole into Aromatase*

The number of docked clusters observed with 1-(Biphenyl-4-ylmethyl)-1H-1,2,4-Triazole for aromatase produced five different clusters (Table II). The sixth run had the lowest binding energy of -14.72 kcal/mol. There was no polar contact between 1-(Biphenyl-4-ylmethyl)-1H-1,2,4-Triazole and aromatase. It was observed that the residues Phe134, Thr310 and Leu477 were taking part in van der Waals interactions (Table III).

*Docking of Anastrozole into Aromatase*

Docking simulation of anastrozole into aromatase resulted in two distinct conformational cluster having eight and two clusters of conformers (Table II).

Fifth run had the lowest energy among all other docked conformations with the binding energy of -14.37 kcal/mol.

In this docked complex, there were two polar contacts involving Thr310 and Ser478 residues at 3.25 Å and 3.51 Å respectively. In addition to polar interactions, residues Arg115, Phe134, Trp224 and Met374 were involved in van der Waals interactions further stabilized the ligand (Table III).

*Docking of 2-{5-[(1H-1,2,4-Triazol-1-yl)methyl]biphenyl-3-yl}-2-methylpropionitrile into Aromatase*

The docked models of clusters of 2-{5-[(1H-1,2,4-Triazol-1-yl)methyl]biphenyl-3-yl}-2-methylpropionitrile had four different clusters with second run having the lowest binding energy of -14.37 kcal/mol (Table II). There were two polar contacts observed between 2-{5-[(1H-1,2,4-Triazol-1-yl)methyl]biphenyl-3-yl}-2-methyl-propionitrile and Ala306, Thr310, Leu372 and Leu477 at 3.30 Å, 3.19 Å, 2.78 Å and 2.74 Å respectively. The van der Waals interactions with ligand were observed in the residues of Trp224, Ser478, Val370, Phe221, Phe134 and Met374 (Table III).

The summary of docking results for andostenedione and top five ligands into protein human aromatase having lowest binding energy is shown in Table II. As shown in Table III, it was observed that nine of the twelve different ligand molecules participated in polar interactions with residues Met374, Arg115, Asp309, Ala306, Thr310, Leu372, Val369 and Leu477 in aromatase which is in accordance with the literature (40). The molecular descriptors for all ligands were calculated using the web server MODEL (41). All ligands satisfied the Lipinski's rule of five for potent inhibitors except Gossypetin and Myricetin which had 6 hydrogen bond donors. Interestingly we found by calculating the molecular descriptors that most of the inhibitors have no hydrogen bond donors.

***Conclusions***

The current study was undertaken to investigate the binding mechanism of known aromatase inhibitors, flavonoids, herbal compounds and compounds having biphenyl motif with known $IC_{50}$ values to the human placental aromatase enzyme and to understand the actual binding modes and the variation in binding affinity of these inhibitors to experimentally-solved aromatase structure. We determined the energetically favored docking sites for the inhibitors and the results explain that the number of distinct conformational clusters found with each ligand varies from one to five. Each distinct conformational cluster has varying number of conformers for aromatase enzyme (Table II-showing docking summary of natural substrate along with top five ligands), indicating that the binding-specificity of each ligand is varying in aromatase. Further, the polar contacts make important contributions to the interactions between ligand and the enzyme. From the frequency of residue's occurrence in the polar contacts, it is evident that Arg115, Met374, Thr310 and Leu477 play an important role interaction with the inhibitors. Potential inhibitors should ideally interact strongly with above mentioned residues. The molecular basis for the enzyme's androgenic specificity and unique catalytic mechanism could be supportive for developing next-generation aromatase inhibitors. It was observed that there were maximum of four polar contacts formed between aromatase and the inhibitors used (Table III). Besides polar interactions, direct van der Waals interactions were also taking part in the stabilizations of inhibitors binding with the side chains of residues Arg115, Ile133, Phe134, Phe221, Trp224, Ala306, Thr310, Val370, Val373, Met374 and Leu477 in aromatase. An ideal aromatase inhibitor would fit the catalytic site of aromatase optimally and would thus interact only with aromatase. Anastrozole (Arimidex), Fadrozole (Afema) and Letrozole (Femara) are currently used as selective potent inhibitors. Anastrozole had the lowest binding energy among the four FDA approved drugs used in

the study and hence claims its effectiveness in using it as an effective inhibitor. A promising perspective is that flavone and flavone derivatives showed effective binding with aromatase with much lower binding energy. But still all these complexes with aromatase were less stable as compared to the natural substrate androstenedione and aromatase complex which had the lowest binding energy of -17.15 kcal/mol among all other ligands studied.

**Table IV**
Molecular properties of the docked ligands.

| S. No. | Molecules | Physical chemistry properties | | Constitutional descriptors | | | |
|---|---|---|---|---|---|---|---|
| | | Hydrophobic alogP | Molecular polarizability | No. of rings | Mw | H-donor | H-acceptor |
| 1 | Aminoglutethimide | 1.6756 | 25.5050 | 2 | 232.2777 | 3 | 4 |
| 2 | Anastrozole | 4.4386 | 33.2240 | 2 | 293.3655 | 0 | 5 |
| 3 | Fadrozole | 2.6213 | 25.8020 | 3 | 223.2726 | 0 | 3 |
| 4 | Letrozole | 4.2224 | 31.8740 | 3 | 285.3023 | 0 | 5 |
| 5 | Flavone | 1.9382 | 28.076 | 3 | 222.2383 | 0 | 2 |
| 6 | Isoflavone | 2.7147 | 28.076 | 3 | 222.2383 | 0 | 2 |
| 7 | Gossypetin | 0.3338 | 31.8980 | 3 | 318.2347 | 6 | 8 |
| 8 | Liquiritigenin | 3.1157 | 27.3660 | 3 | 256.2529 | 2 | 4 |
| 9 | Myricetin | 0.3338 | 31.8980 | 3 | 318.2347 | 6 | 8 |
| 10 | 2-{5-[(1H-1,2,4-Triazol-1-yl)methyl]biphenyl-3-yl}-2-methylpropionitrile | 4.7685 | 36.6150 | 3 | 302.3723 | 0 | 4 |
| 11 | 6-[(1H-1,2,4-Triazol-1-yl)methyl]biphenyl-3-carbonitrile | 3.8543 | 31.1100 | 3 | 260.2928 | 0 | 4 |
| 12 | 1-(Biphenyl-4-ylmethyl)-1H-1,2,4-Triazole | 3.5800 | 29.2580 | 3 | 235.2833 | 0 | 3 |

Our important observation was that most of the effective aromatase inhibitors had no hydrogen-bond donor and have up to five hydrogen bond acceptors (Table IV). Thus, the use of the molecular basis for enzyme-substrate and enzyme-drug interactions could lead to more efficacious intervention of estrogen production. The structure-function studies of aromatase allow us to better understand the reaction mechanism of this enzyme and the binding nature of different classes of inhibitors. This information is critical for the development of new aromatase inhibitors as well as for the identification of novel anti-aromatase phytochemicals for the prevention/treatment of hormone-dependent breast cancers.

***Acknowledgements***

KS was a Summer Faculty Research Fellow in the laboratory of DS under the *Summer Faculty Research Fellow Program 2009* of the *Continuing Education Program* at IIT Delhi. The authors acknowledge the Bioinformatics facility at the Distributed Information Sub Centre, Department of Biochemical Engineering and Biotechnology, IIT Delhi, supported by the Department of Biotechnology (DBT), Govt. of India.

***References***

1. M. J. Murphy, Jr. *Oncologist 3*, 129-130 (1998).
2. R. M. Elledge and C. K. Osborne. *Bmj 314*, 1843-1844 (1997).
3. R. W. Brueggemeier, J. C. Hackett, and E. S. Diaz-Cruz. *Endocr Rev 26*, 331-345 (2005).
4. S. Masamura, H. Adlercreutz, H. Harvey, A. Lipton, L. M. Demers, R. J. Santen, and S. J. Santner. *Breast Cancer Res Treat 33*, 19-26 (1995).
5. E. D. Akten, S. Cansu, and P. Doruker. *J Biomol Struct Dyn 27*, 13-25 (2009).
6. A. M. Andrianov. *J Biomol Struct Dyn 26*, 445-454 (2009).
7. A. M. Andrianov and I. V. Anishchenko. *J Biomol Struct Dyn 27*, 179-193 (2009).
8. A. Borkar, I. Ghosh, and D. Bhattacharyya. *J Biomol Struct Dyn 27*, 695-712 (2010).
9. M. T. Cambria, D. Di Marino, M. Falconi, S. Garavaglia, and A. Cambria. *J Biomol Struct Dyn 27*, 501-509 (2010).

10. E. E. da Cunha, E. F. Barbosa, A. A. Oliveira, and T. C. Ramalho. *J Biomol Struct Dyn 27*, 619-625 (2010).
11. C. Meynier, F. Guerlesquin, and P. Roche. *J Biomol Struct Dyn 27*, 49-57 (2009).
12. S. S. Mohan, J. J. Perry, N. Poulose, B. G. Nair, and G. Anilkumar. *J Biomol Struct Dyn 26*, 455-464 (2009).
13. T. C. Ramalho, M. S. Caetano, E. F. da Cunha, T. C. Souza, and M. V. Rocha. *J Biomol Struct Dyn 27*, 195-207 (2009).
14. J. Sille and M. Remko. *J Biomol Struct Dyn 26*, 431-444 (2009).
15. C. Y. Chen. *J Biomol Struct Dyn 27*, 271-282 (2009).
16. C. Y. Chen. *J Biomol Struct Dyn 27*, 627-640 (2010).
17. C. Y. Chen, Y. H. Chang, D. T. Bau, H. J. Huang, F. J. Tsai, and C. H. Tsai. *J Biomol Struct Dyn 27*, 171-178 (2009).
18. H. J. Huang, K. J. Lee, H. W. Yu, C. Y. Chen, C. H. Hsu, H. Y. Chen, F. J. Tsai, and C. Y. C. Chen. *J Biomol Struct Dyn 28*, 23-37 (2010).
19. H. J. Huang, K. J. Lee, H. W. Yu, H. Y. Chen, F. J. Tsai, and C. Y. Chen. *J Biomol Struct Dyn 28*, 187-200 (2010).
20. E. R. Simpson, M. S. Mahendroo, G. D. Means, M. W. Kilgore, M. M. Hinshelwood, S. Graham-Lorence, B. Amarneh, Y. Ito, C. R. Fisher, M. D. Michael, *et al*. *Endocr Rev 15*, 342-355 (1994).
21. C. Pouget, C. Fagnere, J. P. Basly, A. E. Besson, Y. Champavier, G. Habrioux, and A. J. Chulia. *Pharm Res 19*, 286-291 (2002).
22. H. Adlercreutz. *Environ Health Perspect 103 Suppl 7*, 103-112 (1995).
23. S. Chen, F. Zhang, M. A. Sherman, I. Kijima, M. Cho, Y. C. Yuan, Y. Toma, Y. Osawa, D. Zhou, and E. T. Eng. *J Steroid Biochem Mol Biol 86*, 231-237 (2003).
24. J. Peterson, P. Lagiou, E. Samoli, A. Lagiou, K. Katsouyanni, C. La Vecchia, J. Dwyer, and D. Trichopoulos. *Br J Cancer 89*, 1255-1259 (2003).
25. B. N. Fink, S. E. Steck, M. S. Wolff, J. A. Britton, G. C. Kabat, J. C. Schroeder, S. L. Teitelbaum, A. I. Neugut, and M. D. Gammon. *Am J Epidemiol 165*, 514-523 (2007).
26. D. Ghosh, J. Griswold, M. Erman, and W. Pangborn. *Nature 457*, 219-223 (2009).
27. NCBI-PubChem Compound database (http://pubchem.ncbi.nlm.nih.gov/).
28. S. Karkola and K. Wahala. *Mol Cell Endocrinol 301*, 235-244 (2009).
29. S. Paoletta, G. B. Steventon, D. Wildeboer, T. M. Ehrman, P. J. Hylands, and D. J. Barlow. *Bioorg Med Chem 16*, 8466-8470 (2008).
30. T. Jackson, L. W. Woo, M. N. Trusselle, A. Purohit, M. J. Reed, and B. V. Potter. *Chem Med Chem 3*, 603-618 (2008).
31. H. M. Berman, T. Battistuz, T. N. Bhat, W. F. Bluhm, P. E. Bourne, K. Burkhardt, Z. Feng, G. L. Gilliland, L. Iype, S. Jain, *et al*. *Acta Crystallogr D Biol Crystallogr 58*, 899-907 (2002).
32. G. M. Morris, R. Huey, W. Lindstrom, M. F. Sanner, R. K. Belew, D. S. Goodsell, and A. J. Olson. *J Comput Chem 30*, 2785-2791 (2009).
33. O. Dym, I. Xenarios, H. Ke, and J. Colicelli. *Mol Pharmacol 61*, 20-25 (2002).
34. M. S. Rao and A. J. Olson. *Proteins 34*, 173-183 (1999).
35. G. M. Morris, D. S. Goodsell, R. S. Halliday, R. Huey, W. E. Hart, R. K. Belew, and A. J. Olson. *Journal of Computational Chemistry 19*, 1639-1662 (1998).
36. C. Hetenyi and D. V. Spoel. *Protein Science 11*, 1729-1737 (2009).
37. W. D. Cornell, P. Cieplak, C. I. Bayly, I. R. Gould, K. M. Merz, D. M. Ferguson, D. C. Spellmeyer, T. Fox, J. W. Caldwell, and P. A. Kollman. *Journal of the American Chemical Society 118*, 2309-2309 (1996).
38. G. M. Morris, D. S. Goodsell, R. Huey, and A. J. Olson. *Journal of Computer-Aided Molecular Design 10*, 293-304 (1996).
39. J. C. Cole, C. W. Murray, J. W. Nissink, R. D. Taylor, and R. Taylor. *Proteins 60*, 325-332 (2005).
40. P. P. Roy and K. Roy. *J Mol Model 16*, 1597-1616 (2010).
41. Z. R. Li, L. Y. Han, Y. Xue, C. W. Yap, H. Li, L. Jiang, and Y. Z. Chen. *Biotechnol Bioeng 97*, 389-396 (2007).

*Date Received: August 16, 2010*

***Communicated by the Editor Ramaswamy H. Sarma***